



Technical Sciences  
Academy of Romania  
www.jesi.astr.ro

## Journal of Engineering Sciences and Innovation

Volume 8, Issue 4 / 2023, pp. 415-432

**F. Electrical, Electronics Engineering,  
Computer Sciences and Engineering**

Received 15 September 2023

Accepted 4 December 2023

Received in revised form 23 October 2023

# Developments in Mössbauer Spectroscopy technique

ION BIBICU\*

*Technical Sciences Academy of Romania, Bucharest 030137, ROMANIA*

**Abstract.** The paper presents a large part of the technical developments obtained in the field of Mössbauer Spectroscopy as author or co-author in over 45 years of activity in scientific research. The contributions are mostly made entirely by Roman authors. The developments are exemplified by devices approved for the first time nationally, micro production, patents, experimental arrangements for the first time nationally or internationally, detectors for extending measurements, theoretical and experimental possibility to perform surface measurements for the element europium. The developments are accompanied by numerous scientific papers published in prestigious journals abroad and in the country and have allowed the extension of applications of Mössbauer spectroscopy in physics, chemistry and industry.

**Keywords:** Mössbauer spectroscopy: approved devices, experimental set-ups, detectors, Eu.

## 1. Introduction

Mössbauer spectroscopy [1], [2], [3], [4], [5] represents the recoilless absorption or emission of gamma rays by nuclei embedded in a solid matrix. Its importance lies in a very small width of the gamma ray line, a typical value being of the order of  $10^{-8}$  eV. This results in the ability to examine variations in the energy of nuclear levels resulting from discrete changes in the chemical state or vicinity of the Mössbauer nucleus. These energetic changes are measured by changing the energy of the incident gamma rays on the sample studied by Doppler effect. The Mössbauer spectrum thus consists of representation a number of pulses as a function of Doppler velocities applied (positive and negative) to gamma rays, the velocities corresponding to the addition and decrease of gamma ray energy. Significant recoilless fractions are obtained only for gamma energies less than 150 keV. Mössbauer measurements at room temperature are only possible for 3

---

\*Correspondence address: ionbibicu10@gmail.com

isotopes:  $^{57}\text{Fe}$ ,  $^{119}\text{Sn}$  and  $^{151}\text{Eu}$ , but as but as the energy of gamma rays increases, there is a need for the source and/or sample to be at low temperatures. The isotope  $^{57}\text{Fe}$  is the most studied. After resonant absorption, the nucleus is deexcited by gamma ray emission or by an internal conversion process in which electrons from the inner layers are emitted. The emission of conversion electrons is accompanied by characteristic X-radiation. The detection of the 3 scattered radiation (gamma rays, X-rays and electrons) allows in-depth studies on solid materials. The emission of conversion electrons is significant for the isotopes  $^{57}\text{Fe}$ ,  $^{119}\text{Sn}$  and  $^{151}\text{Eu}$ .

Normal transmission geometry investigates iron samples with a typical thickness of less than 30 microns. In scattering geometry, coatings and thin films containing the Mössbauer isotope can be studied on the substrate and at different depths. In the case of Fe typical values are: by detecting electron conversion of 7.3 keV, 0 – 250 nanometers CEMS-(Conversion Electron Mössbauer Spectroscopy); X-rays of 6.4 keV, 0 – 20 microns XMS-(X ray Mössbauer Spectroscopy) and gamma radiation of 14.4 keV, 0 – 30 microns GMS-(Gamma Mössbauer Spectroscopy). A Mössbauer spectrometer has 3 parts: system for achieving relative source-sample motion, system for radiation detection and data acquisition, stand for measuring geometry.

Mössbauer spectroscopy has one of its most important features: the ability to perform volume and surface analysis simultaneously. It is a non-destructive technique that can be applied in situ to investigate surfaces of varying thicknesses, from thin films to coatings, without having to remove them from their substrate. It allows chemical, structural and magnetic characterization through a single experiment and can examine surfaces and interfaces at a local atomic scale. On the other hand, the method suffers from lower sensitivity and for real surfaces and interfaces, often requiring long acquisition times. Due to the current growing interest in nanomaterials, catalysis and corrosion, it is expected that Mössbauer surface spectroscopy will be more widely used.

The paper presents a large part of the technical developments obtained in the field of spectroscopy Mössbauer as author or co-author in over 45 years of activity in scientific research. The developments are exemplified by devices approved for the first time nationally, micro production, patents, experimental arrangements for the first time nationally or internationally, detectors for extending measurements, theoretical and experimental possibility to perform surface measurements for the element europium.

## **2. Technical developments**

### **2.1. Approved apparatus**

A portable analyser for rapid quantitative determination of cassiterite ( $\text{SnO}_2$ ), the main material in tin mineral industry, have been constructed as homologated prototype [6], [7]. The analyser is presented in figure 1 and it used the transmission geometry. Its electromechanical transducer (loud speaker type) was driven by a

sinusoidal voltage with a frequency close to resonance frequency of the transducer. The quantities  $N_0$  (transducer at 0 velocity, resonance absorption) and  $N_\infty$  (out of resonance) were recorded in the same analysing time between 5 and 40 seconds. The quantity  $N_\infty$  was recorded only for the part of the sinusoidal voltage for which the off resonance condition was fulfilled. The principle scheme of the analyser was the subject of a patent granted [8]. The tin oxide analyser consists of a measuring head and a control and registration electronics in a separate box. The measuring head is designed to permit a variable distance between the radioactive source and the detector. The weight of the analyser was about 9 kg with possibilities to be used in the geological study of the ground. The  $\text{SnO}_2$  concentration is obtained by using a calibration curve which was plotted by measuring the effect on the samples with a known  $\text{SnO}_2$  content. Were obtained calibration curves near sensibility limit, theoretical estimated. The performances of the analyser were: range of tin concentration in powdered sample 0,05% - 10%; weight of sample 1g; the error at the sensitivity limit was lower than 30% and decreases for the increased tin oxide content; required average time for one measurement: 10-15 minute.

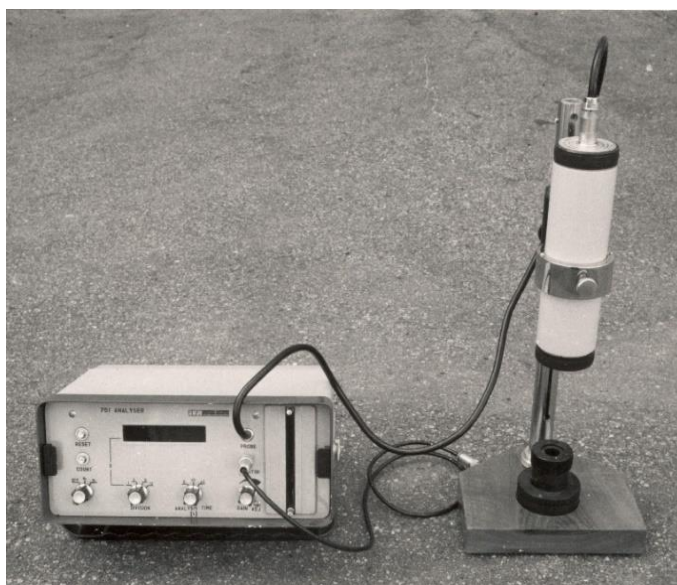


Fig. 1. The view of the analyser for quantitative determination of tin oxide ( $\text{SnO}_2$ ).

A specialized Mössbauer spectrometer was developed for the rapid determination of iron and its compounds in mineral and rock samples (iron analyzer), as homologated prototype. The analyser, shown in figure 2, allows the qualitative and quantitative determination of up to 3 iron compounds (mainly oxides) in a sample or of total iron. The iron compounds under consideration are the main iron minerals: hematite ( $\text{Fe}_2\text{O}_3$ ), magnetite ( $\text{Fe}_3\text{O}_4$ ), siderite ( $\text{FeCO}_3$ ), goetite ( $\alpha\text{-FeOOH}$ ), ilmenite ( $\text{FeTiO}_3$ ), pyrite ( $\text{FeS}_2$ ). The compounds concentrations were obtained by using a calibration curve which was plotted by measuring the effect on

the samples with a known compound content. The device can also be used as a Mössbauer spectrometer operating in constant speed mode. The device, designed for transmission geometry, worked at constant speed and was able to automatically explore any area of the Mössbauer spectrum. The designed analyser combines the versatility of a laboratory Mössbauer spectrometer with the speed and simplicity of a specialized Mössbauer spectrometer. The construction of the iron analyser and the related working methodology were the subject of a patent [9]. The analyser is made in the form of 2 distinct subassemblies: NIM rack (frame) and optical bench stand.

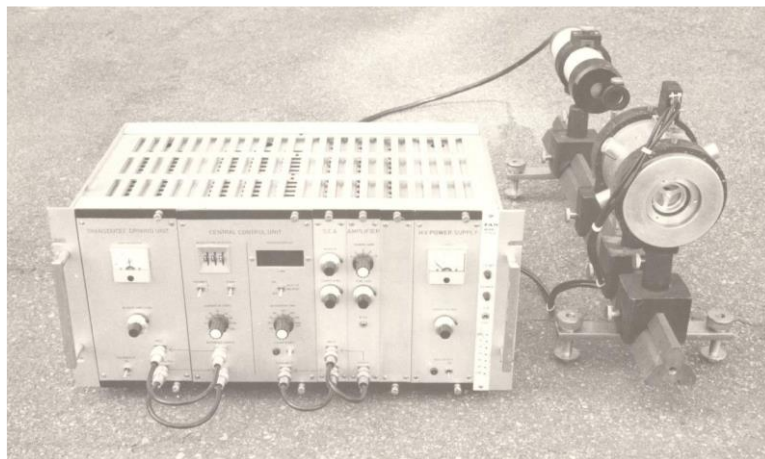


Fig. 2. The overview of the iron analyser.

In the experimentation and valorization of the 2 devices, a general procedure for determining the background in Mössbauer effect measurements [10] was developed and the methodology for performing quantitative determinations of iron (oxides, siderite) and tin (cassiterite) by Mössbauer spectroscopy was established. The background determination method is suitable for thick absorbers in transmission geometry, is relatively insensitive to absorber filter choice and is also applicable to rapid quantitative determinations using calibration curves.

The first 2 devices and the results obtained with them were capitalized through scientific research contracts, 2030/RB/1977; 2030/R1/RB/1978; 2030/R2/1979 1977-1979, on the topic "Development of techniques for the applications of Mössbauer spectroscopy in determining Sn and Fe from rock samples"; contracts financed by the Vienna Atomic Energy Agency (IAEA). The iron analyser was capitalized, by the author as project director, by carrying out a microproduction of 5 analysers during 1979-1984 period, the beneficiaries being the universities of Bucharest, Cluj and Brasov, the Institute of Geology and Geophysics-Bucharest and the Institute for Mining Research-Deva.

The experience gained in the construction of previous devices resulted in the development of a universal Mössbauer spectrometer, a homologated prototype. Under the name of universal Mössbauer spectrometer, the essential part of such a device was realized: the system for achieving the relative source-sample motion

and its associated electronics (function generator, electrodynamic vibrator control electronics, electrodynamic vibrator) [11]. The function generator provides a digitally obtained reference voltage. The device made in NIM system works in transmission geometry and in constant acceleration or constant velocity mode. At the time of its development, its linearity was superior to imported spectrometers and iron analysers. The basic performances of the device are: working mode: constant velocity and constant acceleration; velocity range: 0-10cm/s; number of velocity steps: 256, 512; full linearity for speed range 0-1cm/s:  $\leq 0.5\%$ .

As project director I capitalized on Mössbauer universal spectrometer by carrying out a microproduction of 3 Mössbauer spectrometers between 1983 and 1995 years, the beneficiaries being: IRNE Pitești, University of Cluj-Napoca and IFIN Bucharest.

## 2.2. Experimental arrangements

### 2.2.1. Mössbauer transmission polarizer

A transmission Mössbauer polarizer, which can be attached to any standard Mössbauer spectrometer was achieved [12]. It allows the use of the same transmission geometry for the Mössbauer spectrum and for the Malus curves corresponding to different energies of the polarized gamma ray. The experimental arrangement is shown in figure 3. The Malus curve provide information about the three polarization parameters: intensity, azimuth rotation and eccentricity. The polarizer can be rotated uniformly by a syncromotor with a rotation period in the range of one sweep period for Mössbauer spectrum and the set-up worked as an "automatic polarimeter"

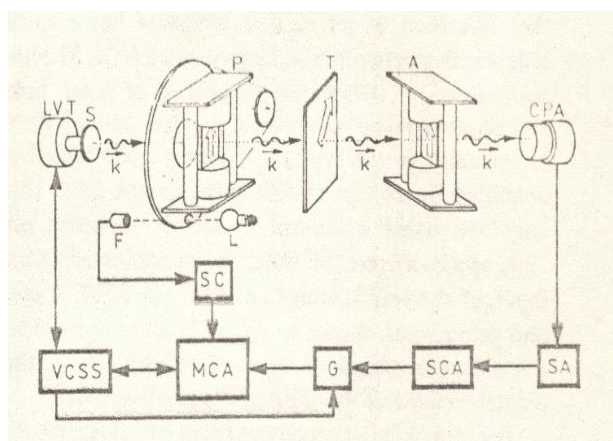


Fig. 3. Experimental arrangement for transmission Mössbauer polarizer

LVT: linear velocity transducer, VCSS: velocity control servo system, CPA: NaI(Tl) crystal photomultiplier assembly, SA: spectroscopy amplifier, SCA: single channel analyser, MCA: multichannel analyser, SC: synchronization circuit, G: gate circuit, S: radioactive source, P: gamma-ray polarizer, T: thick absorber, A: gamma-ray analyser, L: light source, F: phototransistor.

### 2.2.2. Installation for continuous or pulsed application of a radio frequency field

An improved equipment for continuous and pulsed radiofrequency (RF) Mössbauer experiments with an increased capacity to minimize the RF-heating effects was realised [13], [14]. Was possible to obtain spectra in the presence or in the absence of a RF field for similar sample temperatures. The equipment was used successfully to study the influence of a magnetic radiofrequency (RF) field on the properties of ferromagnetic materials, to effect RF treatments on small samples. The equipment, designed as an additional part to an AME-50 Mössbauer spectrometer and a Promeda-01 programmable data acquisition and processing system, is schematically represented in figure 4.

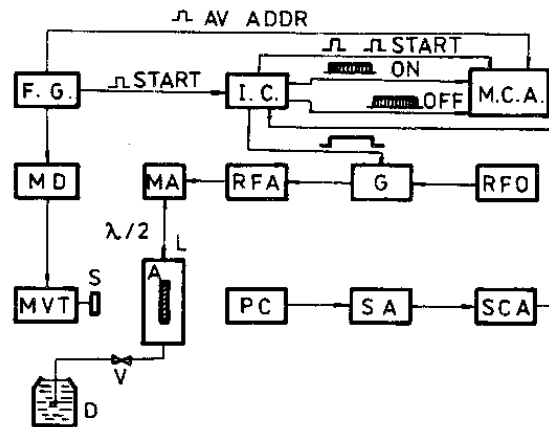


Fig. 4. The experimental set-up of the apparatus for continuous and switched RF Mössbauer experiments

A: sample, L: coil, MA: matching assembly, S: radioactive source, MVT: Mössbauer velocity transducer, MD: Mössbauer drive, FG: function generator, IC: interface circuit, G: gate circuit, RFO: radiofrequency generator, RFA: power amplifier, PC: proportional detector, SA: spectroscopy amplifier, SCA: single channel analyser, MCA: programmable data acquisition and processing system, D: nitrogen dewar flask, V: valve.

The interface circuit (IC) receives the start signals from the function generator (FG) and produces the enable signals for the linear gate circuit (G) and the new start signals for the data acquisition system (MCA). This circuit also routes the signals from a single channel analyser (SCA). By means of the gate circuit, the RF power provided by the radiofrequency oscillator (RFO) and amplified by the RF power amplifier (RFA) is applied continuously or switched to the absorber (A) placed inside the coil (L) of a resonant LC tank circuit. The LC-tank circuit enhances the field strength applied to the absorber and it is commonly used in nuclear magnetic resonance (NMR) studies. The resonant circuit is divided into two parts in order to separate physically the absorber from the rest of electronics. The first part, the matching assembly (MA) consists of two capacitors C and C'. The capacitor C together with inductance (L) forms the resonant tank. The capacitor C' serves to

match the impedance to the  $50 \Omega$  input cable. The second part of the resonant circuit consists of a coil in which the sample is placed. The coil L is such constructed that the attenuation of Mössbauer gamma radiation is minimised. The matching assembly and the coil are linked together by a co-axial cable, one half-wavelength long, designated in figure by  $\lambda/2$ . The temperature of the sample during exposure was measured with an infrared pyrometer. The power amplifier is able to amplify RF signals over the range of frequencies 1-100 MHz up to a power level of 100 W. The quality factor (Q) of the resonant LC tank circuit at the frequency 55 MHz is  $Q=60$ . The RF field in the coil is parallel to the absorber plane and a field intensity from 0 to 20 Oe. Interface circuit assures a variable time between the applications RF field on the absorber. It makes possible to record the Mössbauer spectrum in the presence of the RF field and the second one in the absence of the RF field.

### 2.2.3. Experimental arrangement for the study of the Mössbauer effect in the presence of a strong microwave field

The possibility of nuclear recoil compensation at the absorption of gamma-rays by means of optical photons was considered. The most convenient testing of the two-photon absorption mechanism would be within the frame of Mössbauer spectroscopy, due to the fact that the absorption cross-sections in this case are the highest. An experiment to check the cross-section for recoil-free gamma-ray absorption in the presence of a microwave field was achieved [15]. Schematic drawing of the experimental arrangement for the microwave-Mössbauer resonant absorption is shown in figure 5.

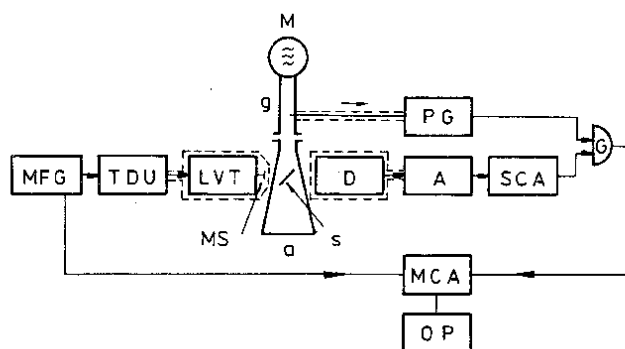


Fig. 5. Schematic drawing of the experimental arrangement for the microwave-Mössbauer resonant absorption

S: sample, MS: Mössbauer source, M: magnetron, MFG: Mössbauer function generator, TDU: transducer driving unit, LVT: linear velocity transducer, D: detector, A: spectroscopy amplifier, SCA: single channel analyser, MCA: programmable data acquisition and processing system, PG: pulse generator, G: linear gate, g: wave guide, a: balanced resistive load, OP: data output/input device.

An experiment of recoil-free 14.4 KeV resonant gamma-ray absorption on polycrystalline  $K_3[Fe(C_2O_4)]3H_2O$  sample exposed to a strong microwave field

was carried out using a constant acceleration Mössbauer transmission spectrometer. The pulsed microwave field was generated by a magnetron (M) with the following characteristics: the power  $P = 1$  MW, the frequency  $\gamma = 3$  GHz, the frequency stability  $\Delta\gamma = 50$  KHz/ $^{\circ}$ C, the pulse width  $\tau = 1$   $\mu$ s and the pulse train frequency  $\gamma_t = 222$ Hz. The sample (S), originated from a single crystal as a finely ground powder, was uniformly pasted by silicon grease on a teflon support making a  $45^{\circ}$  angle toward the reciprocally perpendicular directions of the gamma-beam and the guided field propagation. Two reasons prevailed in the choice of the absorber: a) large enough line width to be detectable on the large Doppler velocity scale demanded by the experiment, b) absence of the internal or magnetic collective phenomena to avoid any acoustic or other undesirable RF effect. The electronics was carefully protected from the influence of the microwave field. A Doppler velocity scale of 30cm/s was used to look for the first-order microwave sideband which was expected to appear at -25.8 cm/s.

The perturbation observed in the spectrum obtained in this experiment can be attributed to a two-photon interaction. Despite experimental difficulties related to microwave power, shielding problems and very low counting rates, experimental data allowed the cross-section of resonant absorption to be estimated in the presence of a microwave field. The obtained value indicated a notable effect of the microwave field on the resonant absorption of 14.4 keV radiation by  $^{57}\text{Fe}$  nuclei.

#### *2.2.4. Installation for the study of Rayleigh scattering of Mossbauer radiation*

Due to the extraordinary high resolution of the Mössbauer effect, the Rayleigh scattering of the Mössbauer radiation can be used to separate elastically and inelastically scattered radiation from crystals not containing Mössbauer isotope. Also it permit to investigate lattice instabilities and structural phase transitions induced by the softening of an optical mode in solids. The relative complexity of the equipment required to perform Rayleigh scattering of Mössbauer is a barrier to the routine use of this technique. These experiments are difficult essentially due to low brilliance of Mössbauer sources. The block diagram in figure 6 presents the final equipment. [16], [17]. There are very few such equipment in the world and for Romania was an opening. The set-up represented a long colaboration between our institue and Horia Hulubei Nationl Institute for R&D in Physics si Nuclear Engineering. Our institute offered Mössbauer spectrometer and Mössbauer expertise.

The equipment for Rayleigh scattering of Mössbauer radiation is similar to a X-ray diffractometer with a Mössbauer source instead the X-ray tube. It consists of three main parts: a goniometer, a Mössbauer spectrometer and a personal computer. The goniometer (G), similar to those used in X-ray precision diffractometer, realizes the measuring geometry. On the goniometer are mounted the electromagnetic vibrator (V) with the Mössbauer source (S), the scatterer probe (P), the nuclear resonance absorber (A), the detector (D). The Mössbauer source was 26mCi of  $^{57}\text{Co}$  diffused into rhodium matrix. The incident and scattered beams are collimated by lead collimators ( $C_1$  and  $C_2$ ) with constant vertical divergence and variable horizontal



divergences. For incident beam the horizontal divergence can be varied between  $0.5^\circ$  and  $2.8^\circ$  using different apertures.

The absorber was an iron enriched  $^{57}\text{Fe}$  (30 atomic %) in a rhodium matrix: 12 microns thickness and 15 mm diameter. The sample and the source can be moved independently and in  $(\theta, 2\theta)$  manner by a stepping motor (SM). A personal computer (PC) controls the orientation of the probe, the Doppler movement and realizes the acquisition of the amplitude spectra and Mössbauer spectra by means of three new cards: SMC, MC, and MCAC. The performances of the system were tested using like scatterers crystals with different mosaic divergences: lithium fluoride LiF(200) with  $10'$  mosaic divergence and pyrolytic graphite C(002) with a higher divergence (up to  $1^\circ$ ).

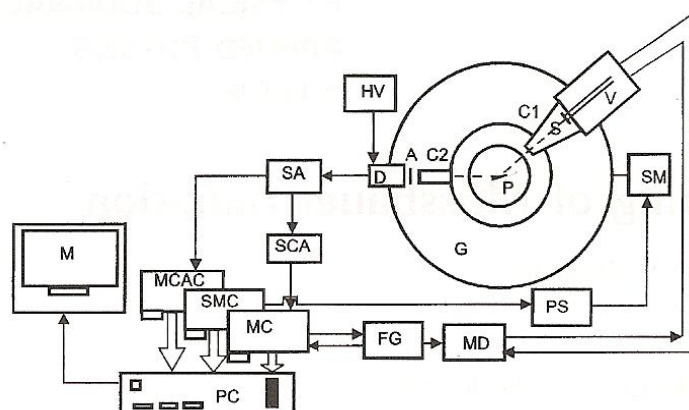


Fig. 6. Block diagram of the PC based set-up for Rayleigh scattering of Mössbauer radiation  
 G: goniometer, V: electromagnetic vibrator, S: Mössbauer source, P: scatterer, A: absorber, C<sub>1</sub>, C<sub>2</sub> collimators, D: detector, HV: high voltage supply, SA: spectroscopy amplifier, SCA: single channel analyser, SM: stepping motor, PS: power supply, FG: function generator, MD: Mössbauer drive, PC: personal computer, MCAC: multichannel analyser card, SMC: stepping motor card, MC: card for acquisition Mössbauer data, M: monitor.

Tests have shown that the installation allows horizontal divergences of the incident beam, variables between  $0.50^\circ$  and  $2.80^\circ$ , smaller than other reported installations, the use of Mössbauer sources of lower intensity and an energy resolution of  $\Gamma = 4.665 \times 10^{-9} \text{eV}$ . The studied Bragg angles are in the range  $0 \div 90^\circ$  and the half width of the diffraction curve for LiF (200) ((BRAGG =  $12.365^\circ$ ) is  $0.6^\circ$ . The study on the pyrolytic graphite C(002) showed a smaller inelastic fraction than that reported for graphite and clearly evidence the contribution of coherent inelastic intensity to the total one. The normal-incommensurate phase transition in  $\text{RB}_2\text{ZnCl}_4$  was studied by Rayleigh scattering of Mössbauer radiation. The discontinuity in resonance effect ( $\varepsilon$ ) proved a stepwise variation of the inelastic component of the scattered radiation. The result was discussed in connection with photon-phonon interaction.

### 3. Detectors for surface studies

There were developed 4 types of proportional gas flow detectors for the detection of backscattered radiation emitted, mainly by the isotope  $^{57}\text{Fe}$ : He-CH<sub>4</sub> detector for simultaneous detection of the Mössbauer effect by conversion electrons and transmitted gamma rays [18] – [20], Ar-CH<sub>4</sub> detector with toroidal geometry for simultaneous detection of the Mössbauer effect by conversion X-rays and transmitted gamma rays, [21], [22] detector assembly for simultaneous measurements by conversion electrons, X-rays and transmitted gamma radiation [19], detector with a variable geometry of the detection space that can be used for the detection of electrons or X-rays depending on geometry and detection gas [23]. All detectors are flow-gas type and operating at room temperature. Their construction permits for all detectors to realize simultaneous transmission and conversion measurements. The background due to photoelectrons is minimised by using low-Z materials as much as possible. The sample holder allows an easy manipulation of a sample outside the detector and sample can always be repositioned in a reproducible manner with respect to the detector body. We have used for detectors an economical shielding which consists of a combination of lead, copper and steel disks. To destroy the characteristic radiation, alternate mounting of the lead, copper and steel disks were used. In order to absorb unfavourable KX-rays from the source, a plexiglas filter is placed in front of the shielding. The detectors were inserted into the Mössbauer ELSCINT AME-20 or AME-50 spectrometers. The spectroscopic chain has been supplemented with additional modules that allow simultaneous accumulation of spectra. To test the performance of the detectors, Mössbauer control measurements were performed on stainless steel test samples (SS 310) for Fe, metal Sn for Sn and Eu<sub>2</sub>O<sub>3</sub> for Eu. The studied samples are part of the detector body and are at potential 0 (mass).

The electron detectors were made using 2 variants in the arrangement of the anode wire: a circle around the sample [18], [19] and parallel and equidistant lines in front of the sample [20], [23]. The second variant shows better performance. The drawing corresponding to this variant is shown in Figure 7 [20], [23].

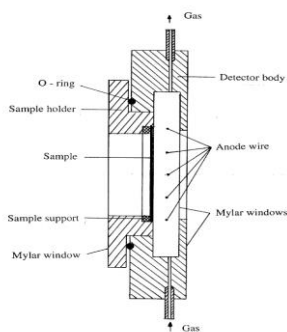


Fig. 7. Cross-section through detector used for simultaneous detection of transmitted electrons and gamma radiation.

The X-ray detector for conversion and transmitted gamma radiation [21] has a toroidal shape of the detection space and shows low efficiency for Mössbauer gamma radiation. The resonant effect can be optimized by an appropriate choice of anode voltage and filter. His design was simpler than other similar detectors described in the literature. A cross-section of this detector is given in figure 9. Subsequently, the toroidal X-ray detector [21] was optimized in terms of mass bonds and the use of a filter to attenuate KX-ray radiation from the source, and a spectacular improvement in the amplitude and Mössbauer spectra was achieved [22]. The improvement in amplitude spectra is illustrated in figures 8a and 8b.

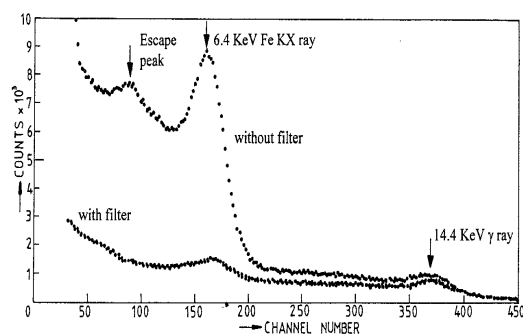


Fig. 8a. Amplitude spectra without optimization of ground bonds with and without filter.

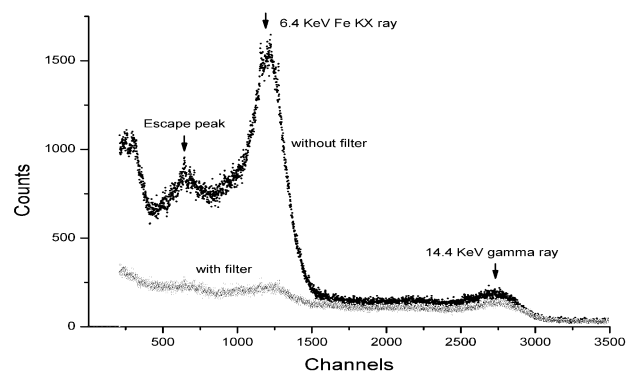


Fig. 8b. Amplitude spectra after optimisation of ground bonds with and without filter.

The detector assembly for simultaneous measurements by electron conversion, X-ray conversion and transmitted gamma radiation [19] consists mainly of 2 gas flow detectors combined together. The sample to be measured is mounted inside the smaller detector designed for electron conversion detection [19]. The larger detector [21] is used to detect X-rays emitted by the sample and passing through the electron detector. The assembly has a low efficiency for radiation of 14.4 keV.

Its construction and mode of operation are simpler than other similar detectors described in the literature. Figure 9 shows the cross-section through this detector

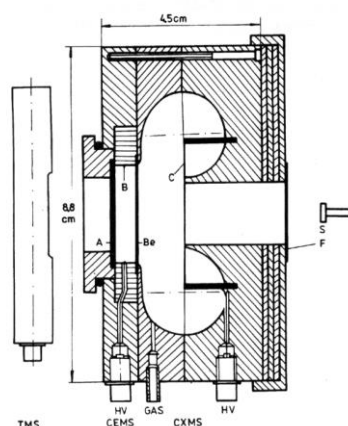


Fig. 9. The detector assembly for simultaneous conversion electron, conversion X-ray and transmission Mössbauer spectroscopy

S: radioactive source, F: filter for X-ray, A: sample, Be: beryllium window, B: anodic wire for electrons, C: anodic wire for X-ray, HV: high voltage connectors, GAS: gas input/output, CEMS: electrons detector, CXMS: X-ray detector, TMS: gamma ray detector.

As a result of the experience gained, a versatile detector was built, suitable for electron or X-ray studies, with all Mössbauer isotopes measurable at room temperature [23]. It has been designed in a cylindrical geometry, similar to that shown in figure 7 and it is presented in figure 10. The detector has the following constructive improvements: the height of the detection volume can be changed within wide limits from 0 to 38 mm, the detection volume can be chosen symmetrically or not in relation to the anode plane, the anode can change easily and reproducibly and thus different configurations of the anode wire can be used. By changing the detection volume and detection gas, measurements can be made by electrons or X-rays. The detector retains the ease of use of the previous ones.

According to our knowledge, the detection of internal conversion X-rays (energy 3.44 – 4.13 keV) emitted by the Mössbauer  $^{119\text{m}}\text{Sn}$  radioactive source and obtaining a Mössbauer spectrum by their detection, using a  $\beta$ -Sn sample, metal foil with the versatile detector [22], was achieved for the first time in the world. The Mössbauer spectrum is represented in figure 11. The spectrum shows the presence of a single line corresponding to  $\beta$ -Sn. The resonance effect,  $\varepsilon = 6\%$ , is smaller than that obtained by transmission geometry (7.9%) but the line width is smaller: 0.91 mm/s versus 0.98 mm/s.

The general characteristics of the detectors are: solid detection angle:  $2\pi$  steradians; anode wire: gilded tungsten, with diameters  $15 \div 50$  microns; gas used: 90%He+10%CH<sub>4</sub>, 94%He+6%CH<sub>4</sub> or 99%He+1%C<sub>4</sub>H<sub>10</sub> for electrons; 90% Ar + 10%CH<sub>4</sub> for X-radiation; gas flow:  $0 \div 2$  cm<sup>3</sup>/minute; anode voltage:  $800 \div 1300$  V

for electrons and 1000÷1500 for X-radiation; energy resolution: about 20% for 6.4 KeV Fe KX radiation. An abstract dedicated to these detectors was published in the database journal of the World data Center Mössbauer [24].

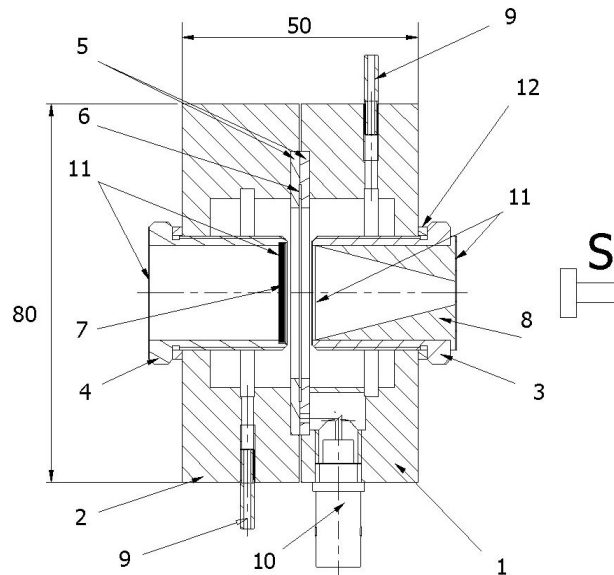


Fig. 10. The cross section of the versatile flow-gas proportional counter  
 1 and 2 main parts of the counter, 3: input piece, 4: sample holder, 5: teflon insulator, 6: anodic ring,  
 7: sample, 8: collimator, 9: gas connection, 10: high voltage connector, 11: mylar windows,  
 12: tightness piece, S: Mössbauer source.

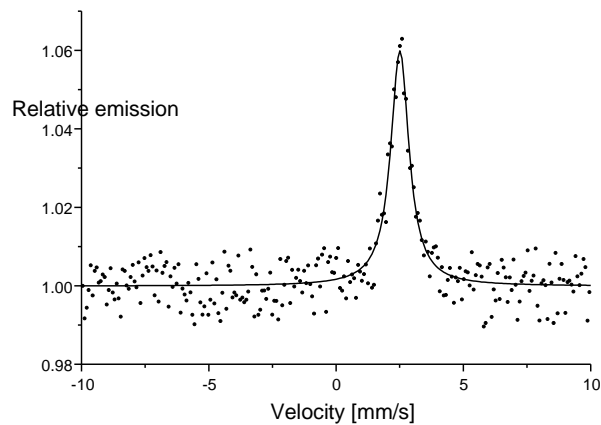


Fig. 11. Mössbauer surface spectrum of  $\beta$ -Sn obtained by conversion X-ray.

#### 4. $^{151}\text{Eu}$ measurements

I demonstrated, for the first time in my opinion, theoretically and experimentally the possibility of making surface measurements on samples containing the isotope  $^{151}\text{Eu}$ , by electrons, practically for the same depth as for isotopes  $^{57}\text{Fe}$ ,  $^{119}\text{Sn}$  [25].

Initially, we highlighted an amplitude spectrum with an electron detector for a  $\text{Eu}_2\text{O}_3$  sample. Surprising because data from the website of the International Mössbauer Center did not show the presence of electrons in radiation emitted after deexcitation of level 21.54 keV of the excited state of the isotope  $^{151}\text{Eu}$ . Consulting another site: <http://ie.lbl.gov/toi/xray.asp> site, managed by Firestone, an author of leading books in the field [26], I found that  $^{151}\text{Eu}$  emits Auger electrons. Their energies are close to those of electrons emitted by the Mössbauer isotope  $^{57}\text{Fe}$ .

An amplitude spectrum corresponding to the Auger electrons emitted by deexcitation of the 21.54 Kev level of  $^{151}\text{Eu}$  is shown in figure 12.

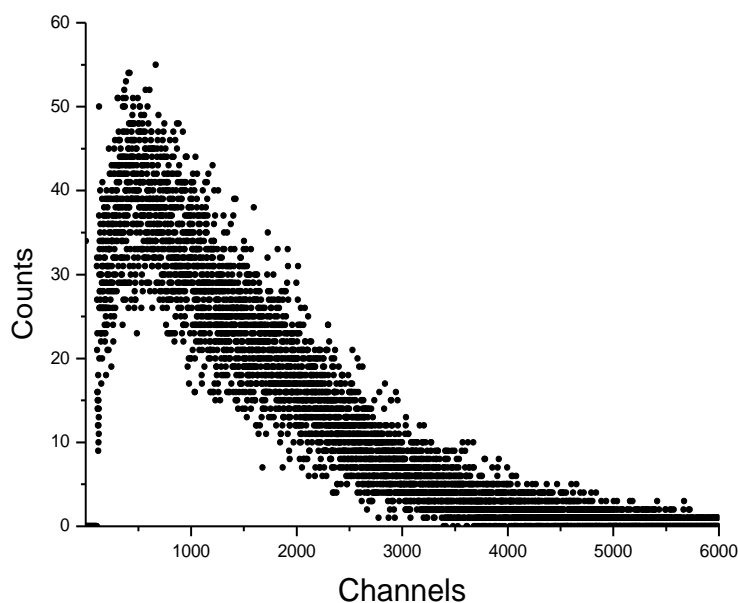


Fig. 12. Pulse height spectrum  $\text{Eu}_2\text{O}_3$  with  $^{151}\text{Sm}$  source, thickness of the detection volume: 4 mm.

Figure 13 compares Mössbauer surface and transmission spectra obtained for the same sample ( $\text{Eu}_2\text{O}_3$ ) with  $10\text{mg}/\text{cm}^2$  thickness. A larger resonance effect and a smaller line width are achieved in the backscatter geometry relative to the transmission geometry. The parameters obtained in the back-scattering geometry, the resonant effect ( $\epsilon$ ) =  $23.69 \pm 0.05\%$ , the line width ( $w$ ) =  $2.56 \pm 0.03$  mm/s are better than those obtained in the transmission geometry:  $\epsilon$  =  $14.57 \pm 0.05\%$ ;  $W$  =  $3.70 \pm 0.03$  mm/s. The spectra were processed with a single Lorentzian lineage

without taking into account the difference in the 2 forms of  $\text{Eu}_2\text{O}_3$  and quadrupolar interaction.

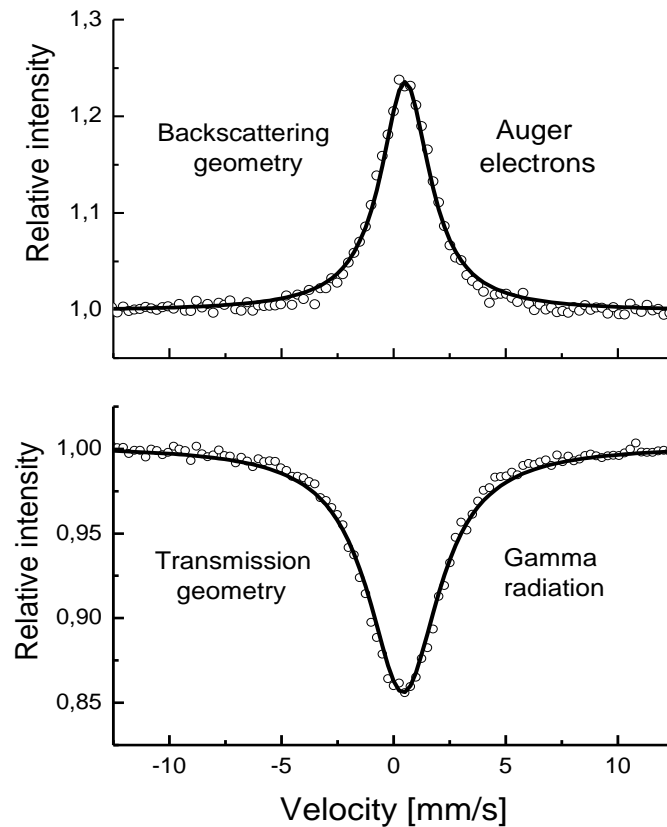


Fig. 13. Mössbauer spectra of  $\text{Eu}_2\text{O}_3$  obtained by Auger electrons (up) and transmitted gamma radiation (down);  $\circ$  data,  $\text{—}$  fit.

## 5. Conclusions

The author presented his contributions to technical developments in achieving and expanding the possibilities of using Mössbauer Spectroscopy in various fields: in economics or in approaching new applied or fundamental research. Developments are proven by patents, microproduction or papers published in prestigious national or international journals.

The development of detectors for surface studies has had the greatest contribution to the expansion of applicative research of all technical developments.

Thus, surface measurements by Mössbauer spectroscopy have contributed to numerous researches: the study of corrosion of carbon steel in dilute ammonia/ammonium solutions: [27], [28], [29], [30], [31], [32], aqueous solutions of hydrochloric acid [33], [34], [35] and aqueous solutions  $H_2SO_4$  [36]; study of corrosion inhibition effect for organic compounds [33], [34], [35], [37], [38]; structural and magnetic properties of films from:  $Fe_{81}B_{13.5}Si_{3.5}C_2$  (Metglass 2605 SC) [39], Cu or Ag implanted with Fe [40], ferrite MnZnTi and NiZn [41]; investigation of effects induced by pulsed radiofrequency (RF) heat treatment, mainly in surface on samples of amorphous substance  $Fe_{81}B_{13.5}Si_{3.5}C_2$  (Metglass 2605 SC) glass [42], [43], [44], [45]; superficial characterisation of alpha-Fe oxides obtained by hydrothermal synthesis [46]; superficial characterization of anatase-TiO<sub>2</sub> doped with  $^{57}Fe$  [47]; nanocrystallization process of amorphous compound  $Fe_{87}Zr_6B_6Cu_1$  [48]; investigation of electrolytic electroplating of Fe-C steel samples with low carbon content [49], etc.

#### References

- [1] Mössbauer R. L., *Nuclear Resonance Fluorescence of gamma Radiation in  $^{191}Ir$* . Z. Physik, **151**, 1958, p. 124-143.
- [2] Maddock A. G., *Moessbauer Spectroscopy: Principles and Applications of the Techniques*, Horwood Chemical, Science Series, Horwood, England, 1997.
- [3] Murad E, Cashion J, *Moessbauer Spectroscopy of Environmental Materials and Their Industrial Utilization*, Kluwer Academic, Netherlands, 2004.
- [4] Bibicu I., *Contribuții tehnice și științifice prin spectroscopie Mössbauer*, Buletinul AGIR, nr. 1, 2019, p. 41-51.
- [5] Bibicu I., *Dezvoltari metodologice in Spectroscopia Mössbauer*, Editori: R. Munteanu, D. Banabic; p. 301-308, ISBN 978-973-713-223-9; 62(063) Lucrările celei de-a Treia Conferințe Nationale a Academiei de Științe Tehnice din Romania Cluj-Napoca, Romania, 2008, p. 301-308
- [6] Barb D., Bibicu I., Prada B, *Analyser for quantitative determination of tin oxide (SnO<sub>2</sub>) by Mössbauer effect*, Rev.Roum.Phys., **22**, 1977, p. 871-873.
- [7] Barb D., Bibicu I., Voicu V., Prada B, *Determinarea cantitativa prin efect Mössbauer a bioxidului de staniu (SnO<sub>2</sub>) din roci*, St.Cerc.Fiz., **29**, 1977, p. 637 – 642.
- [8] Barb D., Prada B, Bibicu I., *Aparat pentru determinarea continutului de SnO<sub>2</sub>*, Brevet de inventie nr. 87846/30.09.1976.
- [9] Barb D., Balanescu M., Bibicu I., *Procedeu si aparat pentru analiza rapida de faza a materialelor feroase*, Brevet de inventie nr. 76459/18.01.1981.
- [10] Bibicu I., *A method for background determination*, Rom. J. of Physics, **39**, 1, 1994, p. 69-73.
- [11] Barb D., Bibicu I., *Sistem de realizare a miscarii relative sursa absorbant pentru spectrometru Mössbauer*, St.Cerc.Fiz., **41**, 1989, p. 881-884.
- [12] Barb D., Rogalski M., Bibicu I., *Transmission Mössbauer polarizer*, Nuclear Instruments and Methods **188**, 1981, p. 469-471.
- [13] Bibicu I, D. Barb D., *Improved equipment for continuous and switched RF Mössbauer experiments*, Meas. Sci. Technol., **7**, 1996, p. 1793-1795.
- [14] Bibicu I., Barb D., *Equipment for continuous and pulsed RF-Mössbauer experiments*, Journal de Physique III, France, **5**, 1995, p. 1865 – 1869.
- [15] Petrascu M, Barb D., Bibicu I., Tarina D., *Recoil-free resonant gamma-ray absorption in  $^{57}Fe$  nuclei in the presence of a strong microwave field*, Hyperfine Interactions, **107**, 1997, p. 247-255. (Gamma Ray Laser volume).
- [16] Enescu S. E., Bibicu I., Zoran V., Kluger Al., Stoica A. D., Tripadus V., *An equipment for Rayleigh scattering of Mössbauer radiation*, The European Physical Journal Applied Physics, **3**, 1998, p. 119-122.



- [17] Kluger A., Enescu S. E., Bibicu I., Ciortea C., A. Enulescu A., *Mössbauer acquisition system for Rayleigh scattering experiments*, Rev. Sci. Instrum., **74**, 6, 2003, p. 3035-3038.
- [18] Bibicu I., Rogalski M. S., Voiculescu Gh, Nicolescu G, Barb D., *Proportional counter for conversion and transmission Mössbauer spectroscopy*, Rev. Roum.Phys., **37**, 1992, p. 315-317.
- [19] Bibicu I, Rogalski M. S., Nicolescu G., *A detector assembly for simultaneous conversion electron, conversion X-ray and transmission Mössbauer spectroscopy*, Meas. Sci. Technol., **7**, 1996, p. 113-115.
- [20] Bibicu I., Rogalski M. S., Nicolescu G., *An improved proportional counter for conversion and transmission Mössbauer spectroscopy*. Rom. J. Phys., **45**, 1-2, 2000, p. 89-97.
- [21] Bibicu I., Rogalski M. S., Nicolescu G., *Toroidal proportional detector for conversion X-ray and transmission Mössbauer spectroscopy*, Nuclear Instruments and Methods in Physics Research B 94, 1994, p. 330-332.
- [22] Bibicu I., *An improvement of the toroidal proportional detector for Mössbauer spectroscopy* Editors: E. Ceanga, C. Fetecau, M. Modiga, D. Ganea Proceedings of The X<sup>th</sup> edition of the Conference: "THE ACADEMIC DAYS OF A.S.T.R", Galati, Romania, 2015, ISSN 2066-6586, p. 226-229.
- [23] Bibicu I., Nicolescu G., Cretu C., *A versatile gas-flow proportional counter for Mössbauer spectroscopy*, Hyperfine Interactions, **192**, 1, 2009, p. 85-91.
- [24] Bibicu I., *Proportional counters for conversion Mössbauer spectroscopy and transmission Mössbauer spectroscopy*, Mössbauer Effect Reference and Data Journal, **27**, 10, December 2004 issue, Mössbauer Instrumentation Abstracts section, page 2.
- [25] Bibicu I, *Comments on <sup>151</sup>Eu Surface Mössbauer Spectroscopy*, Eur. Phys. J. Appl. Phys., **62** (2013) 11302(3 pages).
- [26] Browne E, Firestone R. B, *Table of radioactive Isotopes*, John Wiley & Sons, New York, S.U.A., 1986.
- [27] Bibicu I., Samide A., Preda M., *Steel corrosion in diluted ammoniac solutions studied by Mössbauer spectrometry*, Mat. Lett., **58**, 2004, p. 2650-2653.
- [28] Samide A., Bibicu I, Rogalski M., Preda M., *Surface study of the corrosion of carbon steel in solutions of ammonium salts using Mössbauer spectrometry*, J. Radioanal. Nucl. Chem., **261**, 2004, p. 593-596.
- [29] Samide A., Bibicu I, Tutunaru B., Preda M., *Studiul suprafeței oțelului-carbon corodat în ape industriale care contin NH<sub>3</sub>/NH<sub>4</sub>Cl utilizând spectrometria Mössbauer*, Rev. Chim-Bucharest, **56**, 2005, p. 850-853.
- [30] Samide A., Bibicu I, Rogalski M., Preda M, *A study of the corrosion inhibition of carbon-steel in diluted ammonia media using 2-mercapto-benzothiazol (MBT) by Mössbauer spectrometry*, Acta Chim. Slovenica, **51**, 2004, p. 127-136.
- [31] Samide A., Bibicu I, Rogalski M., Preda M, *Surface study of the corrosion inhibition of carbon steel in diluted ammonia media using N-ciclohexil-benzothiazole-sulphenamida*, Corros. Sci., **47**, 2005, p. 1119-1127.
- [32] Samide A., Bibicu I, Rogalski M., Preda M, *Studiul inhibării coroziunii oțelului-carbon cu etilentiouree în soluții de clorură de amoniu utilizând spectrometria Mössbauer*, Rev. Chim-Bucharest, **54**, 2003, p. 927-931.
- [33] Patru A., Bibicu I., M. Agiu M., M. Preda M., B. Tutunaru B., *Mossbauer Spectroscopy study on the corrosion inhibition of carbon steel in hydrochloric acid solution*, Mater. Lett., **62**, 2008, p. 320-322.
- [34] Samide A., Bibicu I., Turcanu E., *Corrosion inhibition of carbon steel in hydrochloric acid using n-acetyl p-aminobenzene sulphonamide*, Rev. Chim-Bucharest, **60**, 2009, p. 564-567.
- [35] Samide A., Bibicu I., Turcanu E., *Surface analysis of inhibitor films formed by N (2hydroxybenzylidene) thiosemicarbazide on carbon steel in acidic media*, Chem. Eng. Commun., **196**, 2009, p. 1008-1017.
- [36] Bibicu I, Moasil G. C., Barb D., Romanescu M., *Mössbauer technique for investigation the action of an anorganic inhibitor of Corrosion*, Rev.Roum.Phys., **20**, 1975, p. 531-535.
- [37] Samide A., Bibicu I., *A new inhibitor for corrosion of carbon steel in hydrochloric acid solution*, Rev. Roum. Chem., **54**, 2009, p. 33-43.

- [38] Samide A., Bibicu I., *Kinetics corrosion process of carbon steel in hydrochloric acid in absence and presence of 2- (cyclohexylaminomercapto) benzothiazole*, Surf. Interface Anal., **40**, 2008, p. 944-952.
- [39] Rogalski M. S., Jackson T. J., Bibicu I., Palmer S. B., *Deposition of  $Fe_{81}B_{13.5}Si_{3.5}C_2$  films by excimer laser ablation and their structural investigation*, J. Phys. D Appl. Phys., **27**, 1994, p. 2167-2170.
- [40] Pereira de Azevedo M. M., Sousa J. B., Mendes J. A., Almeida B. G., Rogalski M. S., Pogorelov Yu. G., Bibicu I., Redondo L. M., da Silva M.F., Jesus C. M., Marques J. G., Soares J. C., *Magnetization and magnetoresistance in Fe-ion-implanted Cu and Ag thin films*, J. Magn. Magn. Mater., **173**, 1997, p. 230-240.
- [41] Amado M. M., Rogalski M., Guimaraes S. L., Sousa J. B., Bibicu I., Welch R. G., Palmer S. B., *Magnetic properties of NiZn and MnZn ferrite films deposited by laser ablation*, J. Appl. Phys., **83**, 1998, p. 6852-6854.
- [42] Rogalski M., Bibicu I., *Surface short range order induced by RF annealing  $Fe_{81}B_{13.5}Si_{3.5}C_2$  glass*, Mater. Lett., **13**, 1992, p. 32-34.
- [43] Bibicu I., Rogalski M. S., Nicolescu G., *Transmission and conversion electron Mössbauer investigation of  $Fe_{81}B_{13.5}Si_{3.5}C_2$  glass under RF thermal treatment*, Phys. Stat. Sol. (b), **178**, 1993, p. 459-464.
- [44] Rogalski M. S., Bibicu I., Sorescu M., *CEMS investigations of surface hyperfine interactions in  $Fe_{81}B_{13.5}Si_{3.5}C_2$  glass*, Hyperfine Interact., **92**, 1994, p. 1317-1321.
- [45] Rogalski M. S., Bibicu I., *CEMS, CXMS and transmission Mössbauer investigation of the RF isochronal annealing of  $Fe_{81}B_{13.5}Si_{3.5}C_2$  glass*, Physica Stat. Sol (b), **195**, 1996, p. 531-536.
- [46] Diamandescu L., Mihaila-Tarabasanu D., Popescu-Pogriion N., Totovana A., Bibicu I., *Hydrothermal synthesis and characterization of some polycrystalline  $\alpha$  - iron oxides*, Ceramics International, **25**, 1999, p. 689 – 692.
- [47] Grecu M. N., Constantinescu S., Tarabasanu-Mihaila D., Ghica D., Bibicu I., *Spin dynamics in  $^{57}Fe$ -doped  $TiO_2$  anatase nanoparticles*, Phys. Status Solidi B, **248**, 12, 2011, p. 2927-2931.
- [48] Bibicu I., Garitaonandia S., Plazaola F., Apinanz E., *X-ray diffraction, transmission Mössbauer spectrometry and conversion electron Mössbauer spectroscopy studies of the  $Fe_{87}Zr_6B_6Cu_1$  nanocrystallization process*, Journal of Non-Crystalline Solids, **287**, 2001, p. 277-281.
- [49] Bibicu I., Bulea C., Diamandescu L., Rus V., Popescu T., Mercioniu I., *Characterization of surface and interface of Fe-C steel under electrolytic galvanisation*, Proceedings of the Romanian Academy - series A, **19**, 3, 2018, p. 423-430.